ISSN 2410-2547
Опір матеріалів і теорія споруд/Strength of Materials and Theory of Structures. 2026. № 116

UDC 004.94

CONSTRUCTION OF 3D MODELS FOR ADDITIVE MANUFACTURING BASED ON THREE-PERIODIC SURFACES OF THE FOURIER POLYNOMIAL

N.M. Ausheva[1],
Doctor of Technical Sciences, professor

Iu.V. Sydorenko[1],
Candidate of Technical Sciences, assoc. prof.

O.S. Kaleniuk[1],
Candidate of Technical Sciences

Piet Van den Ecker[2],
Research engineer

O.V. Gerashchenko[3],
Candidate of Technical Sciences

[1]*National Technical University of Ukraine "Igor Sikorsky Kyiv Polytechnic Institute", Kyiv, Ukraine*

[2]*Materialise N.V., Technologielaan 15 3001 Belgium*

[3]*Kyiv National University of Construction and Architecture, Kyiv, Ukraine*

DOI: 10.32347/2410-2547.2026.116.120-132

This work proposes an algorithm for Fourier polynomial approximation combined with interpolation that enables the construction of generic tri-periodic surfaces (TPS). In the context of tri-periodic implicit surfaces construction, the interpolating property of the polynomial allows setting the expected function values in points directly, while the approximating property allows for an unlimited number of non-strict guiding points. This enables both explicit and implicit control over the shape of a TPS within the same algorithm. The manufacturability of such surfaces and their applicability in heat exchangers design is also discussed.

Keywords: modeling, 3D model, Fourier polynomial, tri-periodic surfaces, computer-aided design, additive manufacturing, heat exchanger.

Introduction. Most studies in the area of periodic surfaces have lately been focused on triply periodic minimal surfaces. Triply periodic means that they fill the 3D space with a pattern that repeats itself by all three axes, and minimal, by definition, refers to the zero-mean curvature property [1]. These surfaces have been studied extensively along with the numerical methods for their construction [2].

TMPS has been used in tissue engineering [3, 4], where their periodicity property makes them perfect for designing scaffolding structures that help regenerate bone tissue better. Scaffolding structures should have a predesigned porousity, expected smoothness, and they should also be easy to construct computationally. TPMS addresses all of these problems well.

These surfaces have also been extensively used in the design of heat exchangers, where their constant local smoothness, reasonably uniform distribution of inner channels, and high surface-area-to-volume ratio grant them advantages over traditional designs [5–7]. One of the main enablers of TPMS design adoption in heat exchangers was the development in the area of additional manufacturing [8].

Another area of TMPS application would be acoustic absorption [9, 10]. Here, the main benefit of TPMS comes from the ability to form 3D-printable lightweight structures with uniform and predictable acoustic properties.

TPMS-based designs are also employed in structural engineering [11, 12], chemical engineering [13–15], and nuclear energy production [16], where TPMS are used to design fuel cells.

It is worth noting that the minimality of TPMS in the strict mathematical sense means that the surfaces have minimal mean curvature at every point, which is not necessarily optimal for the fluid flow dynamics. For instance, a cylinder, or the inner surface of a tube, is not, strictly speaking, a minimal surface since it has a constant but non-zero mean curvature at any point. It does have zero

Gaussian curvature at any point, though, and this may be important for the flow optimization, but this is not what the surface minimality, in its strict sense, means.

The other sense of surface minimality usually refers to the minimization of the surface area within some constraints. Zhang et al [17] propose to valorize this specific property for the heat exchangers' design. They also challenge the importance of periodicity. What they propose instead is to optimize the heat exchanger surface for the best flow design while keeping it minimal in the sense of minimizing the surface area. This may be counterintuitive since, for better heat exchange, we want to enlarge the surface-area-to-volume ratio and not minimize it, but the authors show that their design, due to optimized fluid flow, is superior to the TPMS-guided design both in terms of pressure drop and constant temperature difference.

In this work, we propose an algorithm for designing triply periodic surfaces that are not minimal, but are still continuous, smooth, regular, and now also governable. By governable, we mean that we can make a surface go through any specific point explicitly and make its implicit function approximate some set of values in predefined points, both at the same time. We argue that this approach is much less restrictive in terms of design possibilities, and the minimality we lose with this approach may not even be beneficial for a wide class of practical applications.

In formal terms, our problem statement is this.

Let's say we have n different points **pin** = ($xin_1, xin_2, \ldots, xin_N$) in N-dimensional space and n scalar values vin assigned to them respectively. We also have m other points **pap** = ($xap_1, xap_2, \ldots, xap_N$) in the same space, and unlike with the first set, some of them may coincide. There are also m scalar values vap assigned to the latter set of points. We want to find an N-ar Fourier polynomial F_p of the given power P, considering $n < (P+1)N$, so the two conditions are met:

$$F_p(\mathbf{pin}_i) = vin_i, \forall_i = 1..n;$$

$$\sum_{j=1}^{m} (F_p(\mathbf{pap}_j) - vap_j)^2 \text{ is a minim.} \quad (1)$$

1. The algorithm of the Fourier combined approximation and interpolation. Let's start from the univariate or 1-dimensional case. The univariative Fourier polynomial is a partial sum of the Fourier series. In its trigonometric form, a polynomial of power p can be written down either as:

$$xF_e(x)=a_0+a_1\cos(x)+a_2\sin(x)+a_3\cos(2x)+a_4\sin(2x)+\ldots+a_{p-1}\cos(\frac{p}{2}x)+a_p\sin(\frac{p}{2}x) \quad (2)$$

or

$$F_0(x)=a_0+a_1\cos(x)+a_2\sin(x)+a_3\cos(2x)+a_4\sin(2x)+\ldots+a_p\cos(\frac{p+1}{2}x). \quad (3)$$

The exact formula depends on whether the degree of the polynomial p is even (2) or odd (3). In this work, we keep the degree of all the polynomials even, but that is not strictly necessary.

To simplify the further notation, let's define a Fourier term f_i for each i degree separately:

$$f_0(x)=1,$$

$$i \bmod 2=1 \Rightarrow f_i(x)=\cos(\frac{i+1}{2}x),$$

$$i \bmod 2=0 \Rightarrow f_i(x)=\sin(\frac{i}{2}x). \quad (4)$$

The whole Fourier polynomial can now be noted as:

$$F(x)=\sum_{i=0}^{P} a_i f_i(x). \quad (5)$$

The Fourier polynomial is a linear function with regard to coefficients a_k, $k = 0..P$. This means that there is one and only one interpolating polynomial of power $P = n$-1 for the n interpolation points, and, in the general case, there is none when $P < n$-1. Since we want our polynomial to be approximating for the set of approximation points, and an interpolating polynomial of power n-1 is unique, and therefore can not be approximating, we demand that $P > n$-1.

ISSN 2410-2547
Опір матеріалів і теорія споруд/Strength of Materials and Theory of Structures. 2026. № 116

Now we should define which coefficients a_k will be dedicated to interpolation. Let's define a set of their indices as c_i (coefficients for interpolation). The power of the set should be strictly equal to the number of interpolating points. E.g., if we have 3 interpolation points, and the power of the polynomial is also 3, then we can have exactly 4 possible sets of coefficients: [0, 1, 2], [0, 1, 3], [0, 2, 3], [1, 2, 3]. Let's call the set of the remaining coefficients' indices c_a (approximation indices). Note that c_a complements the c_i set, so $c_i + c_a = 0..P$. In our example, the possible sets of remaining indices are respectively: [3], [2], [1], [0].

Altogether, there are $(P+1)!/n!$ possible configurations of c_i and c_a. As we show later in this paper with an experiment, the exact choice of the configuration, which indices attribute to interpolation, and which to approximation, is irrelevant for any pragmatic purposes.

If we presume that we already know the coefficient values for coefficients with indices in c_a: aca_j, $j = 1..(p+1-n)$, then the coefficients $aci_j, j = 1..n$, with indices c_i, could be computed by solving a system of linear equations, where every equation follows the $F(x) = y$ for each interpolation point $\mathbf{pin}_i$:

$$\mathbf{aca}=(aca_1,aca_2,...,aca_{p+1-n}),$$

$$\sum_{j=1}^{n} aci_j f_{ci_j}(\mathbf{pin}_i)+\sum_{j=1}^{p+1-n} aca_j f_{ca_j}(\mathbf{pin}_i)=vin_i. \quad (6)$$

Solving this system for the given set of approximating coefficients and complementing the approximating coefficients with interpolating coefficients defines the interpolating and approximating polynomial. Let's call this functional the *Ipol*:

$$\forall_i=1...n:\ \ Ipol:\mathbf{aca}\rightarrow F(x). \quad (7)$$

To define the approximating coefficients, we employ a quasi-Newtonian numeric optimization method, namely BFGS, although the specific choice of the method is mostly irrelevant. The arguments of the optimization are the approximation coefficients: $aca_j, j = 1..(p+1-n)$. And the target function T – is the total square error between the interpolating Fourier polynomial computed for the specific set of approximation coefficients in points $\mathbf{pap}_j$ and the corresponding values $vap_j, j = 1..m$

$$T(\mathbf{aca})=\sum_{j=1}^{m}(Ipol(\mathbf{aca})(\mathbf{pap}_j)-vap_j)^2. \quad (8)$$

The argmin of $T(\mathbf{aca})$ is the approximating coefficients that ensure that the resulting polynomial $Ipol(\mathbf{aca})$ is not only interpolating with regard to points **pin:** $Ipol(\mathbf{aca})(\mathbf{pin}_i) = vin_i$, $i = 1..n$, but also becomes approximating for points **pap**: $Ipol(\mathbf{aca})(\mathbf{pap}_j) \approx vap_j$, $j = 1..m$. An example of such a polynomial is shown in Fig. 1.

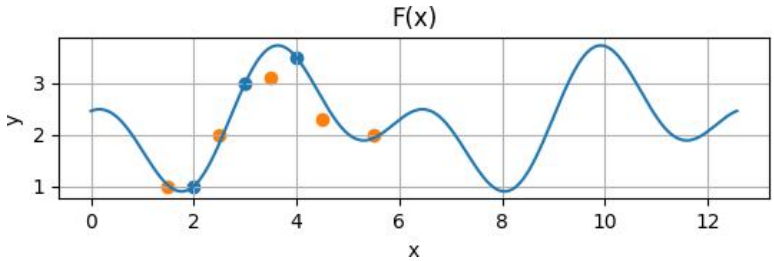

Fig. 1. Fourier polynomial that is both interpolating and approximating

In Fig. 1, we show the polynomial of power 4 that is interpolating for the set of 3 points (shown in blue) and approximating for the set of 5 points (shown in orange). We also show that the polynomial is periodic.

Interestingly, given that the Fourier polynomial is still linear in regard to its coefficients, if the number of approximation points complements the number of interpolation points so that $m+n = p+1$, then the approximation turns into the interpolation as shown in Fig. 2.

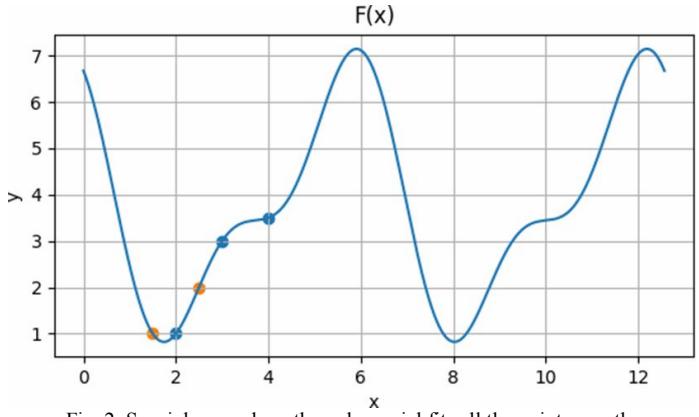

Fig. 2. Special case where the polynomial fits all the points exactly

The uni-variative Fourier polynomial can already be used to model parametric periodic curves [18], but for implicit surface modeling, we need to generalize the algorithm to the N-dimensional case. Now the Fourier polynomial has different powers with regard to different arguments P_i, $i = 1..N$, and the total number of coefficients p defining the polynomial in its full form is then:

$$p=\prod_{i=1}^{N} P_i. \tag{9}$$

The input for the generalized polynomial will be a tuple $x = (x_1, x_2, ..., x_N)$. The output will still be a scalar number.

Given that a single Fourier term for each argument is still $fl_i(x)$, the Fourier polynomial is then the sum of all possible n-ar terms comprised by the product of the unar terms scaled by the respective coefficient. This implies an N-depth nested sum, which is inconvenient for both notation and programming, so instead let's linearize the sum into a single composite index and retrieve the per-argument indices by performing integer division and modulo operations

$$F(\mathbf{x})=\sum_{i=1}^{p} a_i \prod_{j=1}^{N} f_{\frac{i}{\prod_{k=1}^{j-1} P_k \bmod P_j}}(x_j). \tag{10}$$

Let's extract the linearized term $fl_i(x)$

$$fl_i(x)=\prod_{j=1}^{N} f_{\frac{i}{\prod_{k=1}^{j-1} P_k \bmod P_j}}(x_j). \tag{11}$$

And rewrite the $F(x)$ respectively

$$F(\mathbf{x})=\sum_{i=1}^{p} a_i fl_i(\mathbf{x}). \tag{12}$$

The rest of the algorithm goes unchanged. Since we linearized our N-dimensional sum, we can still address the Fourier polynomial coefficients by their indices in this linearized sum. The polynomial is still linear with respect to these coefficients, so we can find the interpolation coefficients by solving the system of linear equations similar to (6):

$$\text{for } i=1...n: \ \sum_{j=1}^{n} aci_j fl_{ci_j}(\mathbf{pin}_i)+\sum_{j=1}^{p+1-n} aca_j fl_{ca_j}(\mathbf{pin}_i)=vin_i. \tag{13}$$

And the values for the approximation coefficients aca_j, $j = 1..(p+1-n)$ can still be obtained by finding a minimum of a target function $T(\mathbf{aca})$ similar to (8):

$$T(\mathbf{aca})=\sum_{j=1}^{m}(Ipol(\mathbf{aca})(\mathbf{pap}_j)-vap_j)^2. \tag{14}$$

Later in this paper, we discuss the computational aspects of such a minimization and show that the minimum of the $Ipol(\mathbf{aca})$ is accessible by a quasi-Newtonian search algorithm from any initial

ISSN 2410-2547
Опір матеріалів і теорія споруд/Strength of Materials and Theory of Structures. 2026. № 116

configuration, so the only drawback of numeric optimization here, compared to the Moore-Penrose quasi-inverse approach, which would usually take place without the interpolating part, is the computational performance.

2. Isosurface construction. For most practical applications, we want to build not just a surface but an enclosing surface of a body in 3D space. A usual technique to do so would be to define a function $S(\mathbf{p})$, where point $\mathbf{p} = (x, y, z)$, representing a quasi-signed-distance field. We conventionally think of points $\mathbf{p}_{\mathbf{in}}$ at which $S(\mathbf{p}_{\mathbf{in}}) < 0$ as being inside the enclosed body, and $\mathbf{p}_{\mathbf{out}}$ at which $S(\mathbf{p}_{\mathbf{out}}) > 0$ as outside the enclosed body, and the isosurface made of $\mathbf{p}_{\mathbf{on}}$ such as $S(\mathbf{p}_{\mathbf{on}}) = 0$ is then the surface we want to construct.

Of course, this is just a convention. Once we have a continuous quasi-signed-distance field function, we may interpret it as the applied problem in hand requires and build a continuous set of isosurfaces $S(\mathbf{p}) = y$. Later in this paper, we'll show how we exploit this property to build an enclosed body of the designed surface's quasi-offset.

In the context of a 3D surface construction, it is reasonable to assume that all polynomial powers P_i, i =1..3 should be same. If it is expected that the target surface deserves a more complex model along one of the axes compared to the others, this equality may be challenged.

To build a surface by the quasi-signed-distance function S represented by an interpolating approximating Fourier polynomial, we need to define the per-argument power of the polynomial P first. The power will affect the shape of the surface, allowing for more variability with higher power, but also hindering control over the shape.

Then we need a set of interpolating points **pin** with the values *vin* for $S(\mathbf{pin}) = vin$. We will use this set to control the surface shape explicitly. The size of this interpolating points set should be less than the degree of the polynomial, power 3 or P^3.

Last but not least, we need a set of approximating points **pap** and the corresponding values *vap*, so the function S will approximate $S(\mathbf{pap}) \approx vap$. The size of this set is unlimited. It can even be less than P^3 when summed with the size of the interpolation points. In this case, the minimum of approximating arguments will lose its uniqueness property, and the shape of the surface will be determined solely by which local optimum the numeric minimizer will stop at, so, while technically not strictly necessary, it's best to keep the total size of interpolating and approximating sets larger than P^3.

For this set of input data, we build the quasi-distance function S as an interpolating and approximating Fourier polynomial according to the algorithm described above. We minimize the error (14) in the space of approximation coefficients while computing the interpolating coefficients from (13) on every iteration.

The combination of interpolation and approximation allows us to have both explicit control over the shape of the surface and to set its behavior by defining arbitrary values in an arbitrary set of points, too. For instance, let's define a pair of helical curves:

$$\begin{array}{l|l} C_1(t)=(x_1(t),y_1(t),z_1(t)), & C_2(t)=(x_2(t),y_2(t),z_2(t)), \\ x_1(t)=\dfrac{\pi}{2}\sin(t), & x_2(t)=\dfrac{\pi}{2}\sin(t+\pi), \\ y_1(t)=\dfrac{\pi}{2}\cos(t), & y_2(t)=\dfrac{\pi}{2}\cos(t+\pi), \\ z_1(t)=t. & z_2(t)=t. \end{array} \tag{15}$$

Now let's define m points on these points, $m/2$ points per curve, each, and space them evenly with respect to the parameter t. For all the points $\mathbf{pap}_i$, $i = 1..m/2$ of the first curve, we assign the same value $vap_i = 1$. For all the points of the second curve, $\mathbf{pap}_i$, $i = m/2+1..m$, we assign $vap_i = -1$. Let's also add one interpolation point $\mathbf{pin}_1 = (0, 0, 0)$ with value $vin_1 = 0$. An isosurface $S(\boldsymbol{p}) = 0$ built with the interpolating and approximating Fourier polynomial, when triangulated for the rendering in a cube $[-2\pi, 2\pi]^3$, looks like in Fig. 3.

What's interesting about this surface is that it is 3-periodic, regular, and anti-symmetric with respect to any axis's 0 point. It also splits the space into exactly two regions that never intersect. The level of control we have allows us to change the latter two properties. For instance, by adding another

interpolating point $\mathbf{pin}_2 = (1, 1, 1)$ and the value $vin_2 = 0$, we can construct an asymmetrical surface (Fig. 4) that keeps all other properties of the original surface.

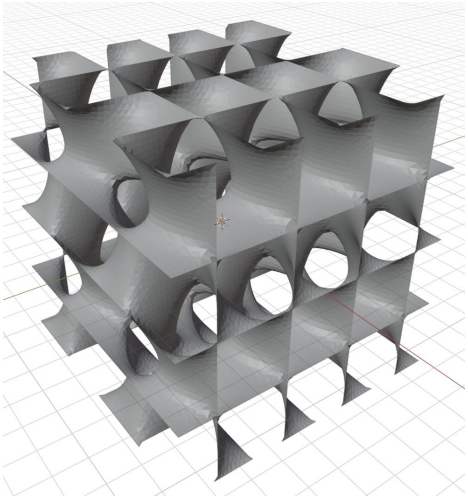

Fig. 3. An example of a 3-periodic surface built with an interpolating and approximating Fourier polynomial

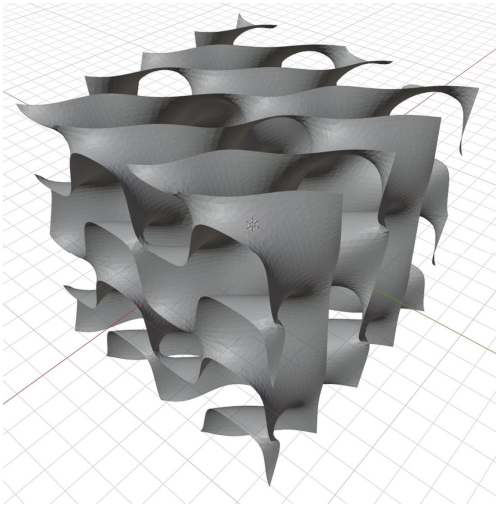

Fig. 4. An asymmetrical version of the 3-periodic surface that splits the space into 2 equal regions

Also, we can choose different values in the approximating points, and this also controls the shape of the surface. For instance, if we set $vap_i = 10$ for $i = 1..m/2$, we will get a new surface that (while being built for all the space, we only show a fragment of it in the figures) will split the space not into 2 regions but into an infinite number of regions. To show this better, let's build our surface within a $[-4\pi, 4\pi]\times[-4\pi, 4\pi]\times[-2\pi, 2\pi]$ parallelepiped (Fig. 5).

As seen from the figure 5, the surface now forms an infinite number of tube-like shapes, each loosely following the helical curve we established with formula (15). Moreover, as the disproportion between approximation values for vap_i, $i = 1..m/2$ and vap_i, $i = m/2+1..m$ rises, the surface converges into an infinite set of zero-width tubes following the given helical curve. In this regard, the surface we propose is one possible generalization of a helical tube, which makes it interesting for practical applications. For instance, this surface gives us enough variability to build anything between a helical coil heat exchanger and a TPMS-like heat exchanger, which are both used in modern engineering in different contexts.

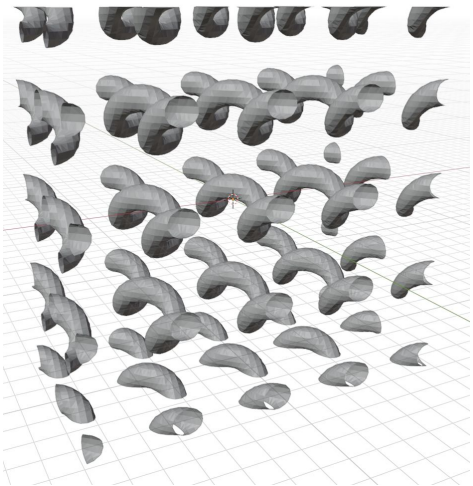

Fig. 5. A surface built with disproportionate approximation values

3. Experimental confirmation that the exact choice of interpolating coefficients is irrelevant. The interpolating and approximating Fourier polynomial is a versatile tool for mathematical modeling. Intuitively, its approximating part should behave like any other linear approximation: there is one, and only one approximating function with a minimal square error, and the function of the approximation square error is, in its turn, convex in the space of linear coefficients. This, however, hasn't been proven mathematically for the combination of interpolation and approximation properties in one function.

Giving a solid mathematical proof for the uniqueness of the approximating and interpolating polynomial and for the convexity of its error function goes beyond the scope of this paper. Instead, we conducted a pair of experiments that show that the properties mentioned above most probably hold.

The first experiment shows that the specific choice of interpolating and approximating coefficients does not affect the resulting polynomial. To back this statement with an experiment, we conducted a

ISSN 2410-2547
Опір матеріалів і теорія споруд/Strength of Materials and Theory of Structures. 2026. № 116

series of algorithm runs in which the choice of n interpolating and m approximating coefficients' indices was defined by a permutation of the range 1..*n*+*m*. For instance, for 3 interpolating coefficients and 2 approximating coefficients, the range is [1, 2, 3, 4, 5], the first set of interpolating coefficients is [1, 2, 3], and the first set of approximating coefficients is [4, 5]. There are exactly 120 permutations of the range, and they include all possible combinations of interpolating and approximating coefficients' indices.

For all the possible configurations of interpolating and approximating coefficients indices, we compute the polynomial coefficients. Then we compare them with the coefficients computed for the initial configuration the sum of squared errors is then recorded.

In our experiments, for the case of 3 interpolating and 2 approximating coefficients, the square error between the initial and all possible configurations of indices did not exceed 7.4e-10.

Due to the fact that the permutation count is $p!$ for the set of p elements, we couldn't repeat the experiment for large numbers of interpolating and approximating coefficients. However, for the combination of 4 interpolating coefficients and 3 approximating coefficients, the square error between the initial and all possible configurations of indices was between 8.3e-17 and 5.1e-8, which confirms the results from the first experiments.

This shows that, apart from some computational error typical for numerical optimization, the resulting interpolating and approximating polynomial built for n interpolating coefficients and m approximating ones is identical for all the possible combinations of approximating and interpolating coefficients indices. Pragmatically, this allows us to always resort to the initial configuration with interpolating coefficients being 1..*n* and approximating: *n*+1…*n*+*m*, and not expect the algorithm to fail or lose precision, or the resulting polynomial to be in any way inferior to the one we would have obtained with any other configurations of coefficients' indices.

The second experiment we conducted shows that the interpolating and approximating polynomial coefficients are discoverable by the BFGS algorithm for any starting point. While this doesn't prove that the function of square error for the approximating points the BFGS is trying to optimize is necessarily convex, it shows that, for all intents and purposes, it behaves as such.

To conduct the experiment, we took the initial data for the generalization of a helical cube (see Fig. 3), and ran the algorithm 1024 times. For each run, the initial point for the BFGS search has been selected randomly, with each coordinate being in the range (-50, 50). Then the error of the approximation for the approximating points has been collected for each run.

In our experiment, the resulting approximation error lies in the range (2.6e-8, 7e-7). There is very little deviation between samples, with a standard deviation of approximately 1.86e-7. This shows that, at least for the class of problems where approximating coefficients outnumber interpolating ones, as is in our case, the optimal approximating coefficients are most probably accessible by the quasi-Newtonian search algorithm, namely BFGS, for any starting point.

This supports the hypothesis that the function of the approximation square error is convex in the space of approximating coefficients for this polynomial. While not mathematically proven, if this is so, this means that in practice, we can rely on any Newtonian or quasi-Newtonian search algorithm to find the approximating coefficients within a reasonable margin of error, and with hyperlinear convexity.

The experiments conducted show that in practice, the specific choice of coefficients' indices is mostly irrelevant for the outcome, and that every choice of starting point for the approximating coefficients search leads to the same result. This boils down the problem of constructing the interpolating and approximating function for any set of input points to the selection of the resulting polynomial's dimensional powers. This is inevitable since, in the context of periodic surfaces modeling, this selection obviously guides the resulting surface shape.

4. Applicability of the algorithm for heat exchangers design. One possible application for the tri-periodic surfaces obtained by the interpolating and approximating Fourier polynomial would be the design of heat exchangers. For instance, as we showed above (see Fig. 5), there is a surface that generalizes helical tubes. Helical coil heat exchangers are already widely used in the industry when, for example, the viscosity and heat propagation properties of the two substances that exchange heat are vastly different. If they are not that different, however, a heat exchanger with the same chambers for both substances can be used. These types of exchangers are usually designed with TPMS. Our approach allows all the configurations in between (see Fig. 6).

The flexibility of the method also allows for the construction of different heat exchangers with desired properties. For instance, if we repeat the algorithm for the helical tube surface but set the initial approximating points to follow the orthogonally oriented sinusoidal curves, e. g.:

$$\begin{aligned} C_1(t)&=(x_1(t),y_1(t),z_1(t)), \\ x_1(t)&=t, \\ y_1(t)&=0, \\ z_1(t)&=-\frac{\pi}{2}\cos(t). \end{aligned} \qquad \begin{aligned} C_2(t)&=(x_2(t),y_2(t),z_2(t)), \\ x_2(t)&=0, \\ y_2(t)&=t, \\ z_2(t)&=\frac{\pi}{2}\cos(t). \end{aligned} \tag{16}$$

Then what we get is a surface that still separates the whole space into two equal parts, but now the section $x = 2\pi k$ for integer k only opens one of the parts, and the section $y = 2\pi k$ - the other part (see Fig. 7).

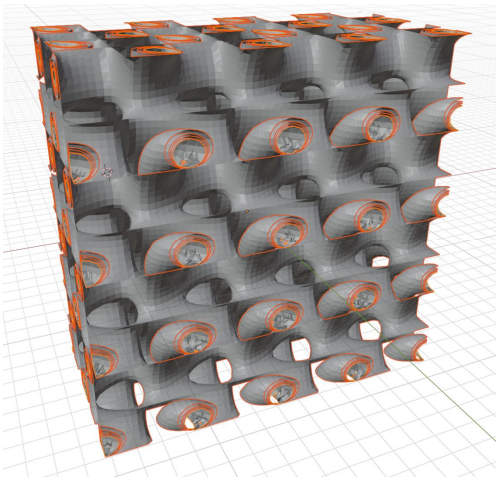

Fig. 6. A set of four surfaces, each with changing values in one of the approximating point sets

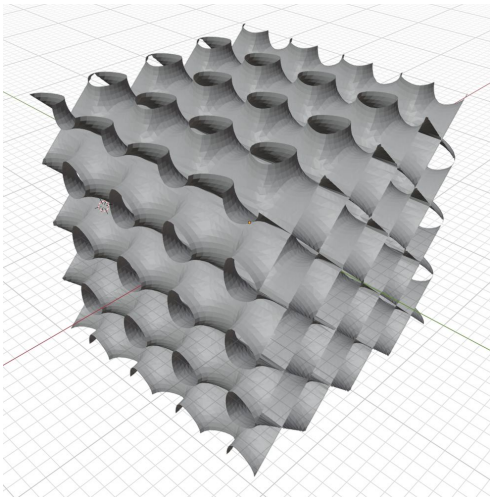

Fig. 7. A 3-periodic surface built around periodic sinusoidal curves with orthogonal axes

Pragmatically, this means that we can use the quasi-offsets of the resulting surface to add thickness to the wall. While doing so, we keep the space separation into 2 non-intersecting parts, and get ourselves a model of a heat exchanger with heat transferring substances having exactly the same flow but in orthogonal direction to each other (see Fig. 8).

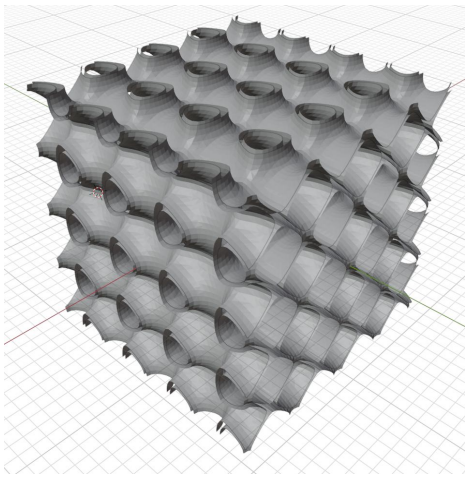

Fig. 8. A model of a heat exchanger fragment built as an offset of a 3-periodic surface

So far, no real heat hardware has been implemented with this type of design, so the reasoning about its practicality is purely theoretical. However, we can already draw some preliminary conclusions based on the geometric properties of the model alone. The model in Fig. 9, when scaled to 37.7 mm per axis, has the bounding box volume of ~53579 mm^3. The surface area of the model is ~38663 mm^2, so the surface-to-volume ratio is 0.72. The volume of the surface offset is ~15954 mm^3 so the relative density of this model as a metamaterial is ~0.3.

The surface area to volume ratio differs with the scale of the model: the more periods the polynomial goes through within a selected volume, the more the surface to volume ratio will be. This, however, compromises the mechanical properties since the walls become thinner too. For this particular model, the offset walls lie within (0.3 mm, 1.5 mm) range.

ISSN 2410-2547
Опір матеріалів і теорія споруд/Strength of Materials and Theory of Structures. 2026. № 116

The width of the channels is then within (1.5 mm, 3.75 mm).

All of this suggests that both the heat conductivity and mechanical properties of this model do not differ drastically from an analogous TPMS surface. But, most importantly, Fourier approximation and inerpolation allows us to design a surface specifically fit for a particular problem.

While the flexibility of the approach allows the construction of intricate surfaces, the practical plausibility of such designs may appear questionable. The method of production, and for these types of surfaces, the most realistic method is 3D-printing, which puts its own constraints on the shape of the surface. For instance, we generally want the internal surface of a heat exchanger to be self-supporting. For this, certain properties should hold, e. g., there should not be large overhangs – fragments of surface with an acute angle to the xy-plane. The exact restrictions depend on the printing technology and the material.

To satisfy these requirements, we can modify the surface explicitly with interpolating points. This is a property TPMS lacks by design, as almost any intervention into the TPMS shape compromises minimality. We argue that printability is more important than minimality, at least in its mathematical sense.

In regard to explicit control, our approach shows more flexible than TPMS.

5. Designed surface readiness for the additive manufacturing. The interpolating/approximating Fourier polynomial method demonstrated in this work enables controlled generation of tri-periodic surfaces with shapes that can be tuned at both global and local scales. This capability is of interest for heat exchanger design, where surface shape and channel architecture govern thermal performance and pressure drop characteristics. Translating such geometries into physical components via additive manufacturing (AM), however, requires an integrated consideration of process-specific constraints, especially for powder bed fusion technologies.

In most industrial contexts, functional heat exchangers are produced in metallic materials using metal AM processes such as laser powder bed fusion (LPBF) or electron beam melting (EBM). In these processes, unsupported overhangs beyond the critical angle typically require temporary support structures, which must later be removed. This poses a significant challenge for enclosed internal channels, as support removal is often infeasible. In contrast, polymer-based laser sintering (LS), as used in the present test samples, does not require supports due to the surrounding unfused powder acting as a build medium. This difference places divergent constraints on surface generation: while polymer LS allows greater freedom for complex internal channels in prototyping, direct metal production demands geometry adapted to self-supporting angles or alternative manufacturing strategies. Examples of LS printed prototypes illustrating this geometric freedom, including perforated cubes and continuous curved channel structures, are shown in Fig. 9.

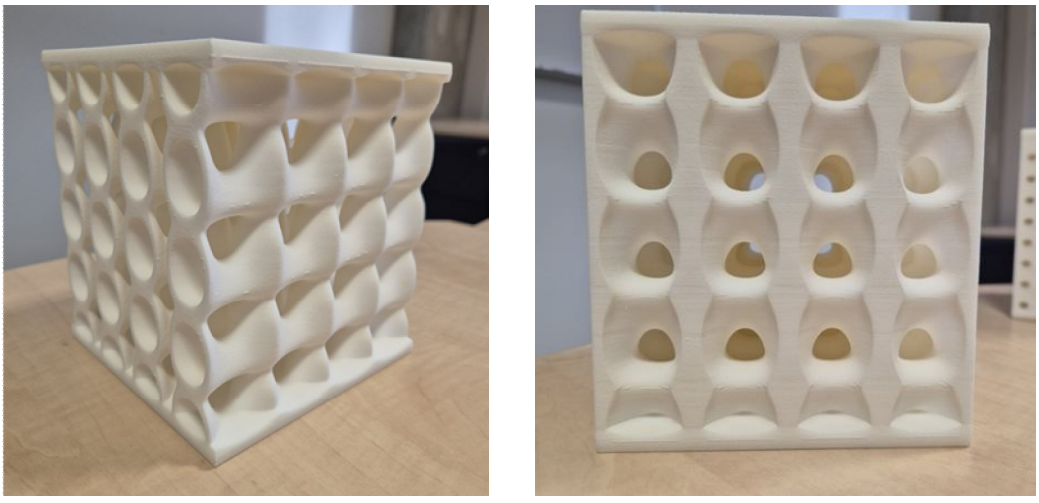

Fig. 9. Laser-sintered TPS-derived cube with continuous curved channels,
manufactured without internal supports (two views)

Surface roughness is a critical consideration across AM processes. As built, internal surfaces possess micro-scale texture governed by powder particle size, energy input, and scan strategy. In fluid channels, this roughness can promote heat transfer in certain flow regimes, but may also incur higher pressure losses. Optimization of roughness - either as built or via post processing - must be matched to the intended operating conditions.

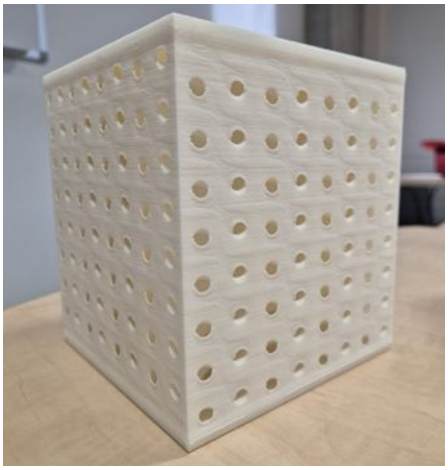

Fig. 10. Example of incomplete surface consolidation linked to irregular laser scan paths and uneven energy delivery

For internal channels in metal heat exchangers, mechanical post-processing is generally impractical, making control of surface texture during the build paramount. The scan strategy plays a decisive role here: Fig. 10 shows an example of surface discontinuities linked to irregular path transitions and suboptimal energy delivery, which can directly impact flow efficiency.

Wall thickness directly influences the balance between surface area to volume ratio and mechanical performance under pressure and thermal cycling. Powder bed fusion accuracy and metallurgical properties constrain minimum viable wall thickness, with typical limits in metals being higher than in polymer LS. The Fourier-based approach supports quasi-offset modelling to modulate local thickness, but this must be reconciled with the minimum feature size that can achieve full density for the specific process and alloy.

Achieving zero porosity is essential for fluid isolation in multi-channel heat exchangers. Incomplete melting or sintering can produce porosities, leading to leakage and reduced mechanical integrity. While AM parameter optimization can mitigate porosity, complex internal geometries may experience varying energy absorption due to scanning patterns. Fig. 11 depicts a cross-section of laser scan paths with mapped energy distribution, highlighting low energy zones between passes as potential porosity sites. Lighter bands indicate high energy regions; darker gaps between paths mark low energy zones prone to incomplete fusion and porosity formation.

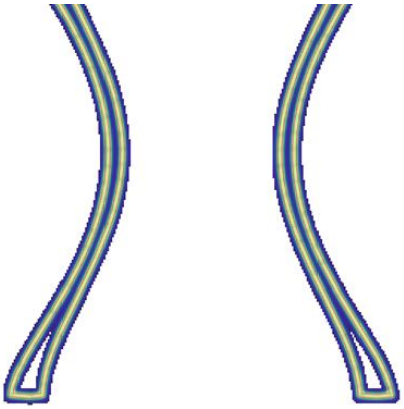

Fig. 11. Cross-section of laser scan paths showing total energy distribution

Such porosity can be directly verified using non-destructive inspection: Fig. 12 presents a computed tomography (CT) scan revealing subsurface voids between layers, confirming the necessity for design stage prevention and post-build evaluation. Dark inclusions indicate incomplete fusion and possible leakage paths.

Channel powder removal is a universal requirement in powder-based AM. Regardless of material, unsolidified powder within enclosed channels must be evacuated post-build. This dictates that channels be continuous, avoid dead-end pockets, and maintain cross-sectional dimensions above the process-specific minimum for powder flowability. In metal AM, powder removal challenges are compounded by finer powders and higher densities relative to polymer LS.

In summary, while the Fourier polynomial approach affords high geometric freedom for tailoring tri-periodic surfaces to thermal applications, its adoption in functional AM-produced heat exchangers depends on process-aware design. For polymer laser sintering, the absence of support structures permits exploration of intricate internal networks during early-stage prototyping. Transitioning to metal AM requires adaptation of geometries to self-supporting constraints, control of surface roughness and wall thickness within metallurgical limits, assurance of full density, and facilitation of powder evacuation.

ISSN 2410-2547
Опір матеріалів і теорія споруд/Strength of Materials and Theory of Structures. 2026. № 116

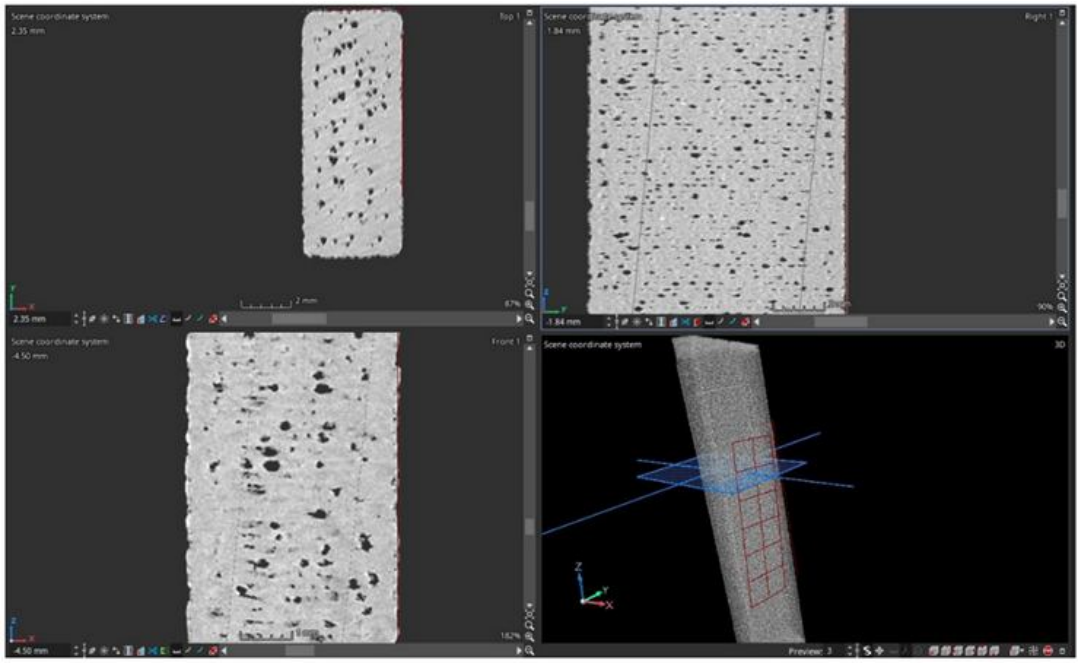

Fig. 12. CT scan cross sections and 3D reconstruction

The integrated use of manufacturing stage data, dynamic analysis [19], geometric prototypes (Figs. 9–10), and non-destructive evaluation (Fig. 12) ensures that the theoretical design advantages of this algorithm can be translated into manufacturable, high-performance components.

6. Conclusion. Combining interpolating and approximating properties in a single Fourier polynomial enables the construction of regular 3-periodic surfaces with two levels of control. The implicit control, given by approximating part, allows us to model the surface with not only points, but also discretized curves, e. g., flow curves. At the same time, explicit control, granted by the interpolating part of the algorithm, allows for shape correction. We believe that this combination makes the algorithm both flexible and governable enough to allow its application for many different technical tasks, modeling 3D-printed heat exchangers being one of them.

REFERENCES

1. Schoen, A.H. (1970) Infinite periodic minimal surfaces without self-intersections, NASA Technical Note, Report No. NASA-TN-D-5541.
2. Karcher H., Polthier K. (1996) Construction of triply periodic minimal surfacesPhil. Trans. R. Soc. A.3542077–2104 http://doi.org/10.1098/rsta.1996.0093
3. Wakjira Y., Cioni A., Lemu H. G. (2025) Current status of the application of additive-manufactured TPMS structure in bone tissue engineering. Progress in Additive Manufacturing. Vol 10, Issue 2, pp 1085-1102. https://doi.org/10.1007/s40964-024-00714-w
4. Giannitelli, S., Accoto, D., Trombetta, M., and Rainer, A. (2014) Current trends in the design of scaffolds for computer-aided tissue engineering, Acta Biomater., vol. 10, pp. 580–594.
5. Mohamed G. Gado, Oraib Al-Ketan, Muhammad Aziz, Rashid Abu Al-Rub, and Shinichi Ookawara. 2024. Triply Periodic Minimal Surface Structures: Design, Fabrication, 3D Printing Techniques, State-of-the-Art Studies, and Prospective Thermal Applications for Efficient Energy Utilization. Energy Technology 12, 5 (March 2024). doi:10.1002/ente.202301287
6. Seo-Hyeon Oh, Chan-Hee An, Bomin Seo, Jungwoo Kim, Chang Yong Park, and Keun Park. 2023. Functional morphology change of TPMS structures for design and additive manufacturing of compact heat exchangers. Additive Manufacturing 76 (Aug. 2023), 103778. doi:10.1016/j.addma.2023.103778
7. Dutkowski, K., Kruzel, M., and Rokosz, K. (2022) Review of the state-of-the-art uses of minimal surfaces in heat transfer, Energies, vol. 15, no. 21, p. 7994.
8. Lihao Tian, Bingteng Sun, Xin Yan, Andrei Sharf, Changhe Tu, and Lin Lu. 2024. Continuous transitions of triply periodic minimal surfaces. Additive Manufacturing 84 (March 2024), 104105. doi:10.1016/j.addma.2024.104105
9. Deshmukh, S., Ronge, H., and Ramamoorthy, S. (2019) Design of periodic foam structures for acoustic applications: Concept, parametric study and experimental validation, Mater. Des., vol. 175, p. 107830.

10. Yang W, An J, Chua CK, Zhou K (2020) Acoustic absorptions of multifunctional polymeric cellular structures based on triply periodic minimal surfaces fabricated by stereolithography. Virtual Phys Prototyp 15(2):242–249. https://doi.org/10.1080/17452759.2020.1740747
11. Sengsri P, Fu H, Kaewunruen S (2022) Mechanical properties and energy-absorption capability of a 3D-printed TPMS sandwich lattice model for meta-functional composite bridge bearing applications. J Compos Sci 6(3):71. https://doi.org/10.3390/jcs6030071
12. Qui, N., Wan, Y., Shen, Y., and Fang, J. (2024) Experimental and numerical studies on mechanical properties of TPMS structures, Int. J. Mech. Sci., vol. 261, p. 108657.
13. Al-Ketan O, Pelanconi M, Ortona A, Abu Al-Rub RK (2019) Additive manufacturing of architected catalytic ceramic substrates based on triply periodic minimal surfaces. J Am Ceram 102(10):6176–6193. https://doi.org/10.1111/jace.16474
14. Baena-Moreno, F.M., Gonzales-Castano, M., Navarro de Miguel, J.C., Miah, K.U.M., Ossenbrik, R., Odriozola, J.A., and Arellano-García, H. (2021) Stepping toward efficient microreactors for CO2 methanation: 3D-printed gyroid geometry, Sustain. Chem. Eng., vol. 9, no. 24, pp. 8198–8206.
15. Lesmana LA, Aziz M (2023) Adoption of triply periodic minimal surface structure for effective metal hydride-based hydrogen storage. Energy 262:125399. https://doi.org/10.1016/j.energy.2022.125399
16. Martin N, Seo S, Prieto SB, Jesse C, Woolstenhulme N (2023) Reactor physics characterization of triply periodic minimal surface-based nuclear fuel lattices. Prog Nucl Energy 165:104895. https://doi.org/10.1016/j.pnucene.2023.104895
17. Zhang, Weizheng and Pan, Hao and Lu, Lin and Duan, Xiaowei and Yan, Xin and Wang, Ruonan and Du, Qiang (2025) DualMS: Implicit Dual-Channel Minimal Surface Optimization for Heat Exchanger Design. Proceedings of the Special Interest Group on Computer Graphics and Interactive Techniques Conference Conference Papers, ACM, pp 1-10, URL: http://dx.doi.org/10.1145/3721238.3730700
18. Ausheva, N. M., Sydorenko, I. V., Demchyshyn, A. A., Kaleniuk, O. S. (2025). Constructing periodic curves with an exponential-algebraic hybrid interpolating polynomial. Computer Science and Applied Mathematics, (1), pp 5-11. https://doi.org/10.26661/2786-6254-2025-1-01
19. Lizunov P. P., Lukianchenko O. O, Geraschenko O. V., Kostina O. V. (2023). Dynamic stability of a hemispherical shell with shape imperfections. Strength of Materials and Theory of Structures, (110), pp. 97-107. https://doi.org/10.32347/2410-2547.2023.110.97-107

Стаття надійшла 22.03.2026

Аушева Н. М., Сидоренко Ю. В., Каленюк О. С., Ван ден Екер П., Геращенко О. В.

ПОБУДОВА 3D-МОДЕЛЕЙ ДЛЯ АДИТИВНОГО ВИРОБНИЦТВА НА ОСНОВІ ТРИ-ПЕРІОДИЧНИХ ПОВЕРХОНЬ ПОЛІНОМУ ФУР'Є

З розвитком 3D-друку стало можливим створення дедалі складніших дизайнів. Конструкції, побудовані на основі три-періодичних мінімальних поверхонь (TPMS), показали себе корисними у різних застосуваннях: тканинній інженерії, акустиці та теплотехниці. Ці конструкції базуються на мінімальних поверхнях, хоча певні дослідження показують, що мінімальність у суто геометричному сенсі не є необхідною і навіть бажаною, для деяких застосувань.

У цій статті пропонується алгоритм апроксимації точкового каркасу поліномом Фур'є який водночас є інтерполяційним для іншого каркасу. Це дозволяє будувати три-періодичні поверхні (TPS). Такі поверхні не є мінімальними, але є більш керованими. У контексті побудови три-періодичних неявних поверхонь, інтерполяційна властивість многочлена дозволяє безпосередньо встановлювати очікувані значення функцій у точках, тоді як апроксимуюча властивість дозволяє мати ще і необмежену кількість точок направляючих. Це дозволяє керувати бажаною формою поверхні за допомогою довільних дискретизованих кривих. Разом це поєднання апроксимації і інтерполяції надає як явний, так і неявний контроль над формою TPS.

Із обома рівнями контролю, можливим стає не тільки створення 3D-моделей тіл, які можуть бути застосовні у всіх сферах де вже використовуються TPMS, а і гарантування того, що їх можливо втілити у матеріалі використовуючи технології адитивного виробництва. Ця стаття розглядає застосування три-періодичних поверхонь на основі полінома Фур'є у конструкції теплообмінників та можливість виробництва конструкцій на основі цих моделей використовуючи процеси лазерного порошкового пласта (LPBF) та плавлення електронного променя (EBM).

Ключові слова: моделювання, 3D-модель, поліном Фур'є, три-періодичні поверхні, комп'ютерний дизайн, адитивне виробництво, теплообмінники.

Ausheva N. M., Sydorenko Iu. V., Kaleniuk O. S., Van den Ecker P., Gerashchenko O.V.

CONSTRUCTION OF 3D MODELS FOR ADDITIVE MANUFACTURING BASED ON THREE-PERIODIC SURFACES OF THE FOURIER POLYNOMIAL

With advances in 3D printing, the construction of increasingly intricate designs has become possible. Metamaterials and devices based on tri-periodic minimal surfaces (TPMS) have proven useful in various applications, including tissue engineering, acoustics, and heat exchange. These surfaces have minimal average curvature at every point, although certain studies show that minimality in a strictly geometric sense is not necessary or even desirable for some applications.

This paper proposes an algorithm for Fourier polynomial approximation combined with interpolation that enables the construction of generic tri-periodic surfaces (TPS), which are not minimal but appear more governable. In the context of tri-periodic implicit surfaces construction, the interpolating property of the polynomial allows setting the expected function values in points directly, while the approximating property allows for an unlimited number of non-strict guiding points. Such points can be obtained by discretizing curves and surfaces. This enables both explicit and implicit control over the shape of a TPS within the same algorithm.

The implicit level of control enables the creation of 3D-models applicable in all fields where TPMS are already in use. The explicit level of control ensures that such models can be produced using additive manufacturing technologies. Not to become too

broad, this particular paper only discusses the applicability of Fourier-based 3-periodic surfaces in heat exchangers design, and printability of the models based on these surfaces in laser powder bed fusion (LPBF) and electron beam melting (EBM) additive manufacturing processes.

Keywords: modeling, 3D model, Fourier polynomial, tri-periodic surfaces, computer-aided design, additive manufacturing, heat exchanger.

УДК 004.94
Аушева Н.М., Сидоренко Ю.В., Каленюк О.С., Ван ден Екер П., Геращенко О.В. **Побудова 3D-моделей для адитивного виробництва на основі три-періодичних поверхонь поліному Фур'є** // Опір матеріалів і теорія споруд: наук.-тех. збірник. – К.: КНУБА, 2026. – Вип. 116 – С. 120-132.
Наведено алгоритм апроксимації точкового каркасу поліномом Фур'є який водночас є інтерполяційним для іншого каркасу. Це дозволяє будувати три-періодичні поверхні маючи як явний, так і неявний контроль над їх формою. Також розглядаються питання адитивного виробництва моделей на основі таких поверхонь і можливість їх застосування при виробництві теплообмінників.
Іл. 12. Бібліогр. 19 назв.

UDC 004.94
Ausheva N.M., Sydorenko Iu.V., Kaleniuk O.S., Van den Ecker P., Gerashchenko O.V. **Construction of 3D models for additive manufacturing based on three-periodic surfaces of the Fourier polynomial** // Strength of Materials and Theory of Structures: Scientific-and-technical collected articles – Kyiv: KNUBA, 2026. – Issue 116. – P. 120-132.
This paper proposes an algorithm for Fourier polynomial approximation combined with interpolation that enables the construction of generic tri-periodic surfaces (TPS), which enables both explicit and implicit control over the shape of a surface. The plausibility of Fourier-polynomial-based models for additive manufacturing is discussed, along with the prospects of using these types of models for the construction of heat exchangers.
Fig. 12. Ref. 19.

Автор (науковий ступінь, вчене звання, посада): доктор технічних наук, професор, завідуюча кафедрою цифрових технологій в енергетиці НТУУ «КПІ ім. Сікорського» АУШЕВА Наталія Миколаївна.
Адреса: 03056 Україна, м. Київ, Берестейський проспект 31, НТУУ «КПІ ім. Сікорського».
Мобільний тел.: +380-95-540-60-35
E-mail: nataauscheva@gmail.com
ORCID ID: https://orcid.org/0000-0003-0816-2971

Автор (науковий ступінь, вчене звання, посада): кандидат технічних наук, доцент, доцент кафедри цифрових технологій в енергетиці НТУУ «КПІ ім. Сікорського» СИДОРЕНКО Юлія Всеволодівна.
Адреса: 03056 Україна, м. Київ, Берестейський проспект 31, НТУУ «КПІ ім. Сікорського».
Мобільний тел.: +38-099-369-39-41
E-mail: suliko6786@gmail.com
ORCID ID: https://orcid.org/0000-0002-1953-0410

Автор (науковий ступінь, вчене звання, посада): кандидат технічних наук, старший викладач кафедри цифрових технологій в енергетиці НТУУ «КПІ ім. Сікорського» КАЛЕНЮК Олександр Сергійович.
Адреса: 03056 Україна, м. Київ, Берестейський проспект 31, НТУУ «КПІ ім. Сікорського».
Мобільний тел.: +38-064-021-45-89
E-mail: o.kaleniuk@kpi.ua
ORCID ID: https://orcid.org/0009-0009-3141-4840

Автор (науковий ступінь, вчене звання, посада): інженер-дослідник «Materialise» N. V. Ван Ден ЕКЕР Піт.
Адреса: 3001 Бельгія, Технологілаан, 15, центр досліджень і розробки, «Materialise» N. V.
Мобільний тел.: 0032486046651
E-mail: Piet.VandenEcker@materialise.be

Автор (науковий ступінь, вчене звання, посада): кандидат технічних наук, старший науковий співробітник, завідувач відділом НДІ будівельної механіки КНУБА, ГЕРАЩЕНКО Олег Валерійович.
Адреса: 03037 Україна, м. Київ, пр. Повітряних Сил, 31, Київський національний університет будівництва і архітектури
Тел.: +38(044)248-30-40
E-mail: olg_guera@ukr.net
ORCID ID: https://orcid.org/0000-0003-1951-4805